Fall 2017

Augmenting Mask-Based Lithography with Direct Laser Writing to Increase Resolution and Speed

Miles Patrick Lim
Bard College, ml8127@bard.edu

Recommended Citation

Lim, Miles Patrick, "Augmenting Mask-Based Lithography with Direct Laser Writing to Increase Resolution and Speed" (2017). *Senior Projects Fall 2017*. 40.
https://digitalcommons.bard.edu/senproj_f2017/40

Augmenting Mask-Based Lithography with Direct Laser Writing to Increase Resolution and Speed

A Senior Project submitted to

The Division of Science, Mathematics, and Computing

At Bard College

By

Miles Lim

Annandale-on-Hudson, NY

December 2017

TABLE OF CONTENTS

LIST OF FIGURES

DEDICATION

This work is dedicated to my grandfather Lowell C. Parode. He always encouraged me to follow my curiosities and enjoy the world around me. I also greatly thank my parents Lynne and Sterling for their love and support.

ACKNOLEDGEMENTS

I want to thank my advisor Chris LaFratta for being an incredible mentor and friend. I could not be more grateful to have been welcomed into his lab and had the opportunity to work with him on the hybrid lithography project. His commitment to his students and contagious love of science inspires me to strive for excellence every day. In addition to being an incredible professor and advisor, our shared interest in books, podcast, and TED talks has changed the way I see the world forever.

I also owe a big thanks to the Bard Chemistry department and all of the professors for making chemistry available and unintimidating. I am constantly in awe of how dedicated our faculty are to their student's in every possible way. We are so lucky to have all of you.

Lastly, I would also like to thank the Bard Research Fund and the Bard Summer Research Institute for funding this work.

ABSTRACT

We present combined direct-laser-writing and UV Lithography in SU-8F and S1813 as a fast and flexible lithographic technique for the prototyping of functional polymer devices and pattern transfer applications. Direct laser writing (DLW), which is performed by focusing a laser through a microscope objective, is a useful alternative method for patterning photoresists with sub-micron resolution. DLW however, can be time consuming if the pattern density is high since it is a serial technique. Typically, dense patterns are made using conventional mask-based UV lithography, but these masks can be quite expensive if the resolution is high and the mask cannot be modified once created. Here, we combine UV lithography using inexpensive transparency masks, which have modest resolution of about 20 μm linewidths, with DLW to create smaller features. By using the laser to augment an inexpensive mask, high resolution prototypes can be created, tested, and modified quickly to optimize a design. Here we show that this Laser Augmented Microlithographic Patterning (LAMP) method works with both positive- and negative-tone photoresists, S1813 and SU-8, respectively. The laser written features can be registered to within 2.2 μm of the mask created features and we demonstrate the applicability of LAMP by fabricating an interdigitated electrode and a microfluidic device that can capture an array of dozens of silica beads or living cells.

1. INTRODUCTION

Conventional mask-based lithography and direct laser writing (DLW) can be combined into a hybrid technique, which compensates for the drawbacks of each. Photolithography using a mask to expose a photoresist to UV light is commonly used for the production of microelectronics but has applications including microelectromechanical systems (Waggoner et. al. 2007), lab-on-a-chip devices (Xia et. al. 1998), and DNA microarrays (LaFratta et. al. 2008). The power of photolithography lies in its ability to pattern large areas at sub-micron resolution in a matter of minutes. Two issues with photolithography are: i) the initial cost of the mask, which can be substantial if the resolution is high; and ii) the rigidity of the mask since it cannot be altered. These issues can make prototyping a new device via photolithography fairly expensive. An alternative patterning method that does not suffer from these issues is direct laser writing (DLW), in which a laser is focused to a point in a photoresist and moved with respect to the sample to generate the pattern. One issue with DLW is the potentially long time required to cover large areas. The method we describe here is a combined lithographic technique that utilizes the large area patterning abilities of mask lithography and the serial patterning of direct laser writing, which together provide high resolution patterns, in a short amount of time, and at a reasonable cost. This combined lithography system can effectively pattern from sub-micron to millimeter resolution with much higher throughput than DLW on its own, while offering more pattern flexibility than plain mask lithography. This can be used as an alternative means for creation of microfluidic masters and for prototyping microelectronics.

Others have also investigated hybrid lithography schemes such as the pairing of UV lithography with of electron beam lithography (EBL) (Rahman et. al. 2010; Nakano et. al.

2016; Potosky et. al. 1981; Carbaugh et. al. 2017; Steen et. al. 2006; Mollard 200; Benistant et. al. 1996; Jonckheere et. al 1995) or nanoimprint lithography (NIL) (Dhima et. al. 2012; Scheer et. al. 2010; Montelius et. al. 2010; Reuther et. al. 2011; Scheer et. al. 2010). For example, Kristensen et. al. report the patterning of SU-8 with EBL followed by UV lithography resulting in features as small as about 100 nm linewidths (Gersborg-Hansen et. al. 2007). While EBL is most frequently used with positive tone photoresists to open areas for depositing metal contacts, this work shows that by combining with UV lithography EBL can also be used to fabricate relief structure for molds. Nanoimprint lithography (NIL) has also been used as the first step in a sequential technique to pattern 500 nm features in SU-8 followed by a UV exposure to make contacts at the 200 μm scale (Skjolding et. al. 2009). These are attractive prototyping technologies that offer rapid pattern generation with fine resolution. The use of direct laser writing as part of a hybrid scheme is less common, but Eschenbaum et. al. 2013 and Muluneh et. al. 2015 devised a hybrid DLW and UV lithography schemes for multi-scale patterning. They created high resolution patterns in three dimensions using an ultrafast laser for two-photon polymerization. The results are impressive showing the fabrication of a miniature 45° mirror to view particles from the side while traveling in a microfluidic channel. Shear and coworkers have also demonstrated a DLW system that uses the mirror array from a projector to quickly transfer a high-resolution pattern, thereby increasing the speed of DLW. Such two-photon systems can be very expensive and somewhat difficult to operate compared to a simple continuous wave diode laser, which is what we report here.

In this work, we present a combined DLW and UV lithography scheme that uses both positive and negative photoresists as a fast and flexible lithographic technique, suitable for wafer scale definition of both millimeter and sub-micrometer scale features. Our method, which we call Laser Augmented Microlithographic Patterning (LAMP), first exposes a photoresist through an inexpensive transparency mask and then adds to that exposure using a DLW system before finally developing the pattern (Figure 1). If one already has a microscope, then it can be readily adapted into a DLW system (LaFratta et. al. 2015). LAMP is fairly low cost, straightforward to perform, and requires only a single photoresist layer and development step. We show that we can register the DLW features to within about 2 μm of the mask alignment marks and can achieve sub-micron linewidths. We envision LAMP to be an attractive alternative to expensive masks for prototyping devices for researchers. We demonstrate two simple proof-of-principle devices, a microfluidic cell trap and an interdigitated electrode (IDE), to show the utility of LAMP.

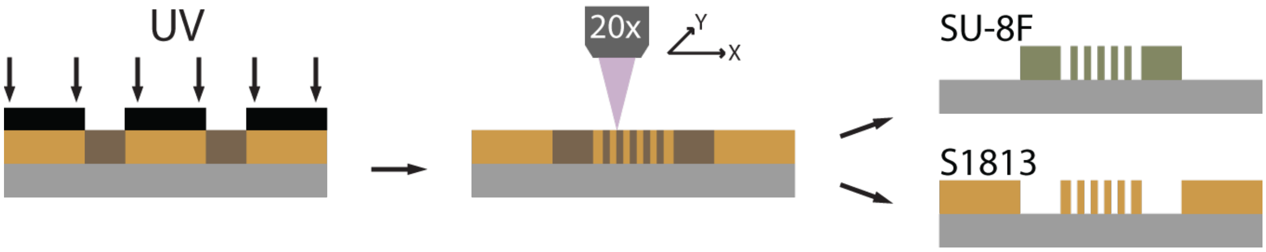

Figure 1: Experimental steps involved in the laser augmented microlithographic patterning (LAMP) procedure for both positive and negative photoresist. The photoresist is first exposed to UV through a transparency mask, then the exposed region changes color, allowing registration for new features to be patterned by direct laser writing (DLW). Development yields positive (S1813) or negative (SU-8F) microstructures that can then be used for additional steps like metal evaporation or molding.

2. EXPERIMENTAL METHOD

2.1 LAMP Procedural Overview

Experimental conditions and the optical components of our system are described in depth in previous publications by our lab (Lafratta et. al. 2015). For positive photoresist, Shipley S1813 (Microchem) was spun on 2” glass wafers to a thickness of approximately 1.5 μm. For negative photoresist, we doped SU-8 2005 (Microchem) with fluorescein in a ratio of 1 mg of fluorescein to 1 mL of SU-8 to yield “SU-8F”. The SU-8F was thoroughly mixed before being spun onto 2” silicon wafers to a thickness of 5 μm. The wafers were soft baked according to their data sheets provided by Michrochem and exposed through a transparency mask to a 100 W mercury lamp (Blak-Ray) for 60 s. The wafers were then mounted onto an inverted fluorescence microscope (IX-71, Olympus), which had a motorized X-Y stage (Proscan III, Prior) coupled to a manual rotation stage (Thorlabs). A 405 nm continuous wave diode laser (OBIS, Newport Corporation) was directed through a custom laser port in the filter turret and focused through a 20X numeric aperture (NA) 0.75 objective onto the sample. The X-Y axis of the exposed mask pattern and the microscope stage were made parallel using the rotation stage, the laser spot was then aligned to a registration point on the exposed mask pattern. The desired power, speed, and focal position along the optical axis (Z-axis) could be adjusted to create lines of varying linewidth. The DLW of the photoresist for S1813 was performed using about 300 nW, while the SU-8F required about 500 μW. These powers were measured before the microscope, but at the sample they were 13% of these values due to reflective loss at the mirror and because the laser overfilled the back aperture of the objective. Following the exposure of the resist in the desired pattern, the sample was submerged in the appropriate developer; S1813 was developed in Microposit

351 for one minute and SU-8F was post baked and developed in propylene glycol monomethyl ether acetate for one minute. Linewidths and registration of patterned features were characterized by scanning electron microscopy, SEM, (MIRA 3, Tescan) for several objective lenses, power, and sample position along the Z-axis.

2.2 Baking, UV Exposure, and Development Testing

The experimental conditions were originally carried out according to their data sheets (Microchem), but because of differences in equipment we optimized the times and temperatures ourselves. Baking temperatures remained at 65°C and 95°C for SU-8F, but were reduced from 115°C to 95°C for S1813. Exposure times between 45 s to 90 s, for both resists, were tested. Additionally, development times between 5 s and 120 s were tested. All baking, exposure, and development tests were performed using the US Airforce Test Mask standard (USAF1951) with features resolution down to 2.19 μm.

2.3 DLW Resolution Testing

DLW of S1813 and SU-8F was tested at various speeds and powers to determine optimal conditions for augmenting mask features. For both resists, six power studies on six individual wafers were prepared and averaged to collected the linewidth data. For negative tone SU-8F, the lines were defined in parallel with two perpendicular lines to help them stand up. Following development, these lines were measured by SEM to determine the linewidth.

2.4 Registration Testing

Registration between the mask exposed pattern and the DLW pattern was tested using a mask having a series of rectangles regularly spaced over 25 mm, that were connected by both horizontal and vertical lines by DLW. Following development, the patterns were imaged by SEM and the position of the laser augmented lines was measured with respect to the center of the target rectangles. When measuring registration data, Δx and Δy were measured at the center (L1,R1) and at the edges (L10,R10).

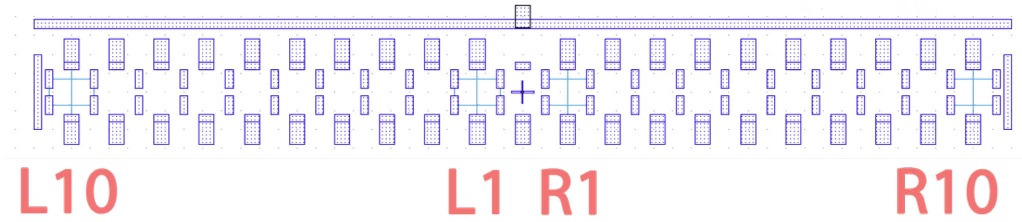

Figure 2: The image above shows the mask pattern (in purple) that was used to test the laser registration (in blue). L10, L1, R1, and R10 indicate where on the wafer the measurement were taken.

2.5 Interdigitated Electrode Fabrication

The fabrication of the interdigitated electrode (IDE) began with a transparency mask drawn in LayoutEditor and was printed on a Mylar transparency by Advanced Reproductions (N. Andover, MA) and was available in 24 hours for $50. The mask had contact leads on the order of 250 µm wide and about a centimeter in length which came together but left a gap of 1.3 mm. In the gap between leads, LAMP was used as previously described with S1813 to add interdigitated lines about 2 µm wide with a spacing of 12.5 µm and with a length of 200 µm. Following development, the samples were placed in a thermal evaporator (Edwards) and 2 nm of Cr was evaporated followed by approximately 50 nm of Au. Liftoff was performed by soaking the sample in acetone for 1 hour followed by gentle stirring, and the final sample was imaged by both optical and scanning electron microscopy.

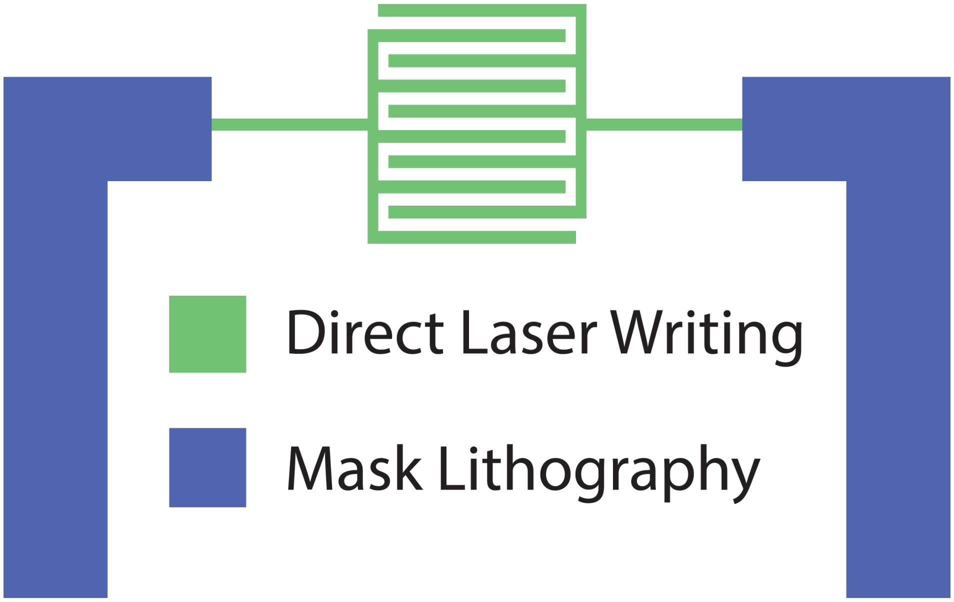

Figure 3: The graphic above show the mask pattern that was used to make the contact wire for the interdigitated electrode test structure.

2.6 Microfluidic Cell Trapping Array Fabrication

The microfluidic designed to trap an array of cells was also made using a Mylar mask with a similar pattern to an IDE except it had lines that were 15 µm wide with 15 µm gaps between them and they were 500 µm long. The Si wafer was spin coated with SU-8F, prebaked, and exposed through this mask. Next, a series of lines were drawn perpendicular to the "IDE" pattern. After post-baking and developing, this master structure was silanized with a fluorocarbon to make it non-stick and polydimethylsiloxane (PDMS) (Sylgard 184, Dow Corning) was mixed, degassed, and cast onto the master. After 1.5 hours at 60°C the PDMS was cut off the master, holes were punched, and the PDMS was placed in a plasma cleaner (Harrick) along with a clean glass slide for 1 minute (LaFratta et. al. 2004). The air plasma oxidized both the PDMS and the glass slide. After they were removed from the plasma cleaner the PDMS was gently placed on the glass slide and placed in a 110°C oven for 10 minutes to irreversibly bond (Duffy et. al. 1998). Tubes were then inserted into the previously punched holes and a dilute solution yeast cells or 5 μm silica beads were flowed into the device. The functional device was positioned on an inverted microscope and images of the array of cells were captured using a CMOS camera (Thorlabs).

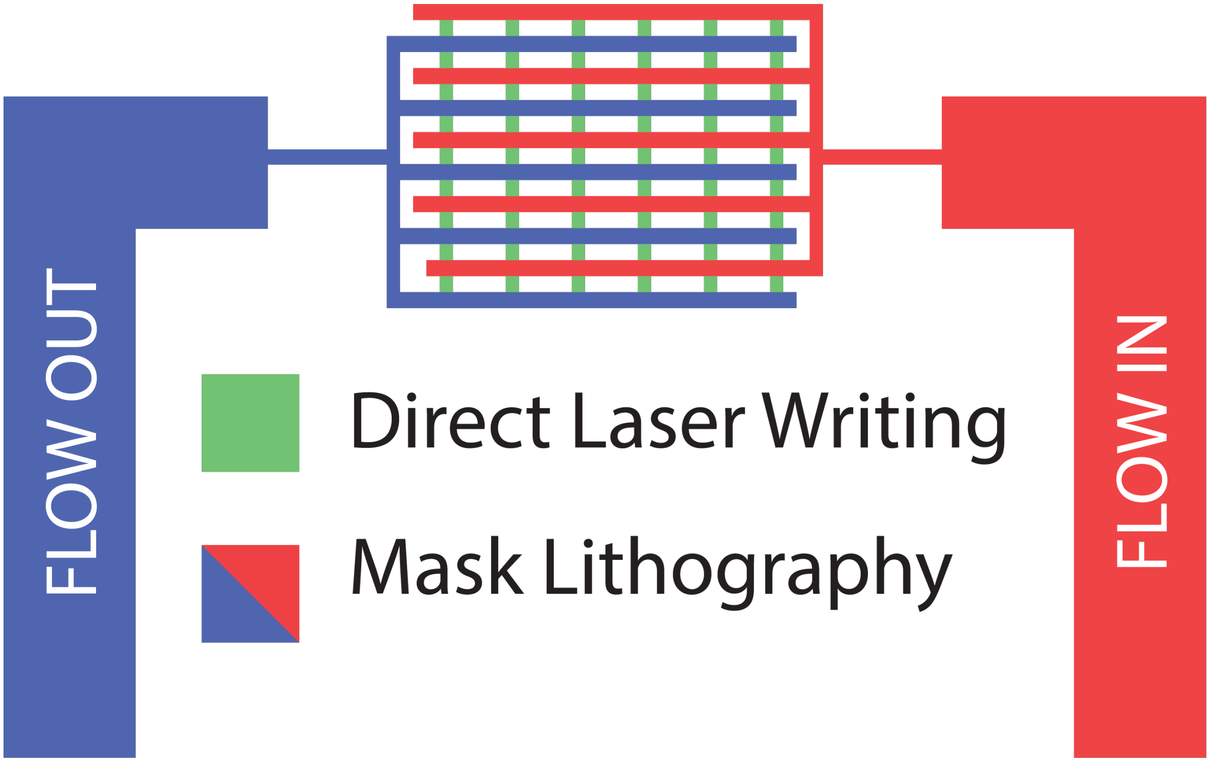

Figure 4: The graphic above shows the mask pattern that was used for the cell trapping microfluidic, and the additional laser patterns added to make the microfluidic master. The scheme also shows the flow in and out of fluid to demonstrate the flow of cells or beads and where they would trap.

3. RESULTS AND DISCUSSION

3.1 The LAMP Method is Dependent on the Photochromism of the Resist

When exposed to UV radiation, both S1813 and SU-8F have photochromic properties resulting in contrast between the exposed and unexposed regions. This contrast enables the DLW system to be aligned with the mask exposed patterns and is critical for LAMP. The photos in Figure. 5 shows both S1813 and SU-8F before and after UV exposure. SU-8 generates a photoacid upon exposure, but shows no color or refractive index change. In order to visualize where the pattern that had been exposed, we doped SU-8 with various concentrations of fluorescein, which is a fluorophore and also a pH indicator. We found that at low concentrations of fluorescein the SU-8F was slightly more yellow in the exposed regions but there was not enough contrast to see the difference between exposed and unexposed regions. If the fluorescein concentration were too high, for example 2 mg/mL, then the contrast was excellent but the developed sample would frequently fall off of the substrate, presumably because the fluorescein interrupted the epoxide polymeric network. We found 1 mg/mL to be ideal for providing enough contrast while maintaining the material properties of SU-8. The SU-8F, which is a clear and colorless, turns bright yellow upon exposure due to the generation of acid and the change in the protonation of the fluorescein molecule in acidic environments, which is yellow (Sjöback et. al. 1995). The S1813 can be seen to photobleach upon exposure turning from clear red to clear colorless. To enhance this color change we used a blue LED as an illumination source on our DLW microscope. The yellow SU-8F lines absorb the blue light and appeared dark indicating where the mask exposure took place.

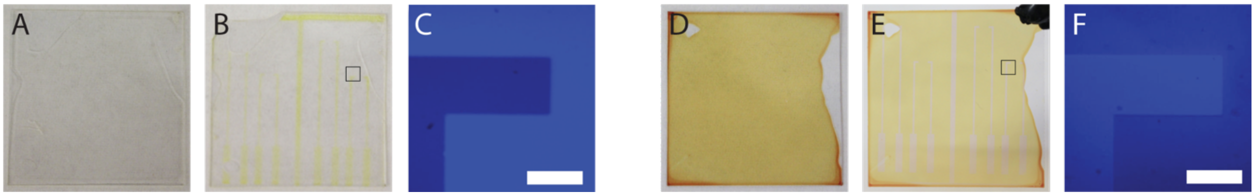

Figure. 5: Both S1813 and SU-8F show a photobleaching/photochromic effect following exposure to UV, which enables registration between features made with a mask and those made with the laser. Images (A) and (B) show 25 mm coverslips coated in SU-8F before and after exposure, respectively. (C) Shows the contrast of SU-8F on the DLW microscope for the area corresponding to the small square in (B). (D-F) are the analogous images for S1813. The scalebars in (C) and (F) are 250 µm.

3.2 The Procedure was Optimized for Reproducible High Resolution Lines

Factors like prebaking time and temperature, UV exposure time, and development time have an impact on the reproducibility of the resolution when working with submicron features. For S1813, the sample was soft baked for 2 minutes at 95°C, exposed for 45 s, and developed for 45 s. This was optimal for the USAF test mask, but for exposing the Mylar mask for the LAMP process an exposure time of 60 s ensured the pattern was defined properly. For SU-8F, the sample was soft baked for 1 min at 65°C and 3 min at 95°C, exposed for 60 s, hard baked for 1 min at 65°C and 3 min at 95°C, and developed for 60 sec.

3.3 The LAMP Procedure Requires Modification of an Inverted Fluorescence Microscope

In order to write accurate laser lines with respect to the mask exposed pattern, the laser and the mask systems need to be squared together. This was achieved with a manual rotation stage (Thorlabs) that was affixed to a custom mount machined to fit inside of the microscope’s 96-well plate holder. This held the sample at the proper focal height, while adding adjustability in theta. Using the contrast between exposed/unexposed photoresist and the rotational stage, the pre-exposed pattern could be adjusted so that it was squared with the X-Y axis of the microscope stage.

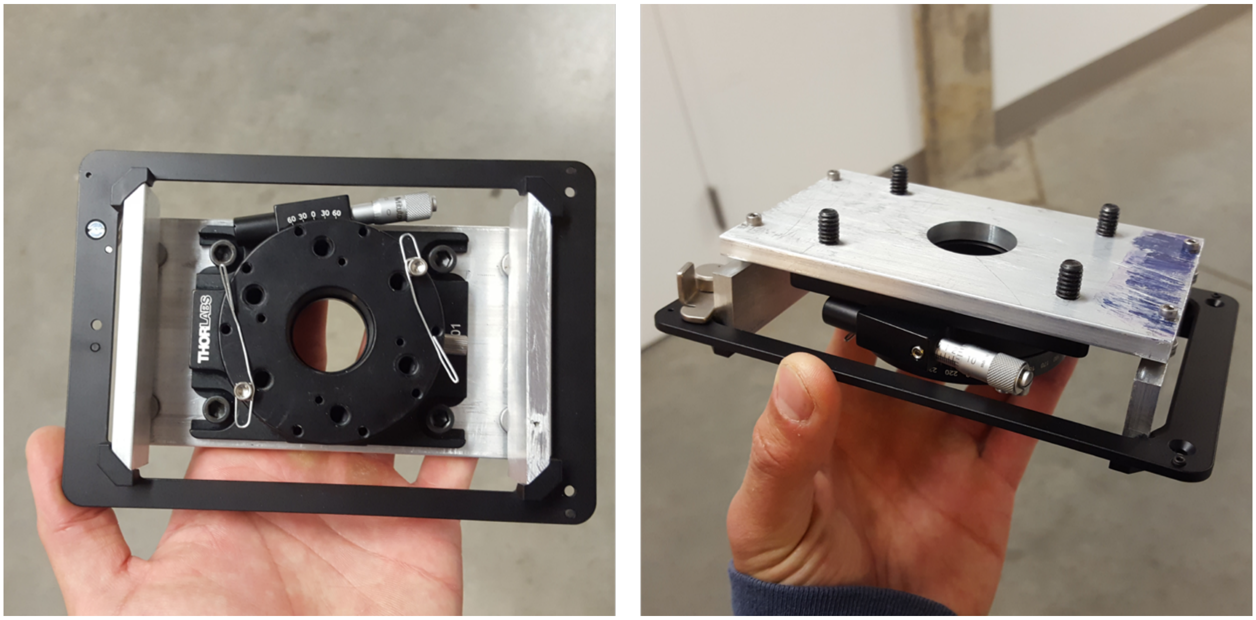

Figure 6: Shows images of the manual rotation stage mounted to a 96 well pate holder for an Olympus IX-71. The left image shows the clips for mounting the sample and the image on the right shows the rotational nob.

3.4 Mask Design

The mask was designed with an array of features to demonstrate the viability of the LAMP technique. The transparency masks was drawn in LayoutEditor and were printed on a Mylar transparency by Advanced Reproductions (N. Andover, MA). The primary designed had two major features: a bar through the middle of the mask, and a centering dot. The 26,000 μm bar was used to square the mask pattern as described above. The centering dot was used to tell the program where the center of the mask was. Once the program knew where the center was and the pattern was squared, we could write laser lines in (x,y) coordinates with respect to the existing mask pattern. The mask also included a series of rectangles which were used for registration (Figures 2 & 7) and a series of test structure features. Additional masks included contact wires for IDEs and the base pattern for the cell trapping microfluidic (Figures 3 & 4).

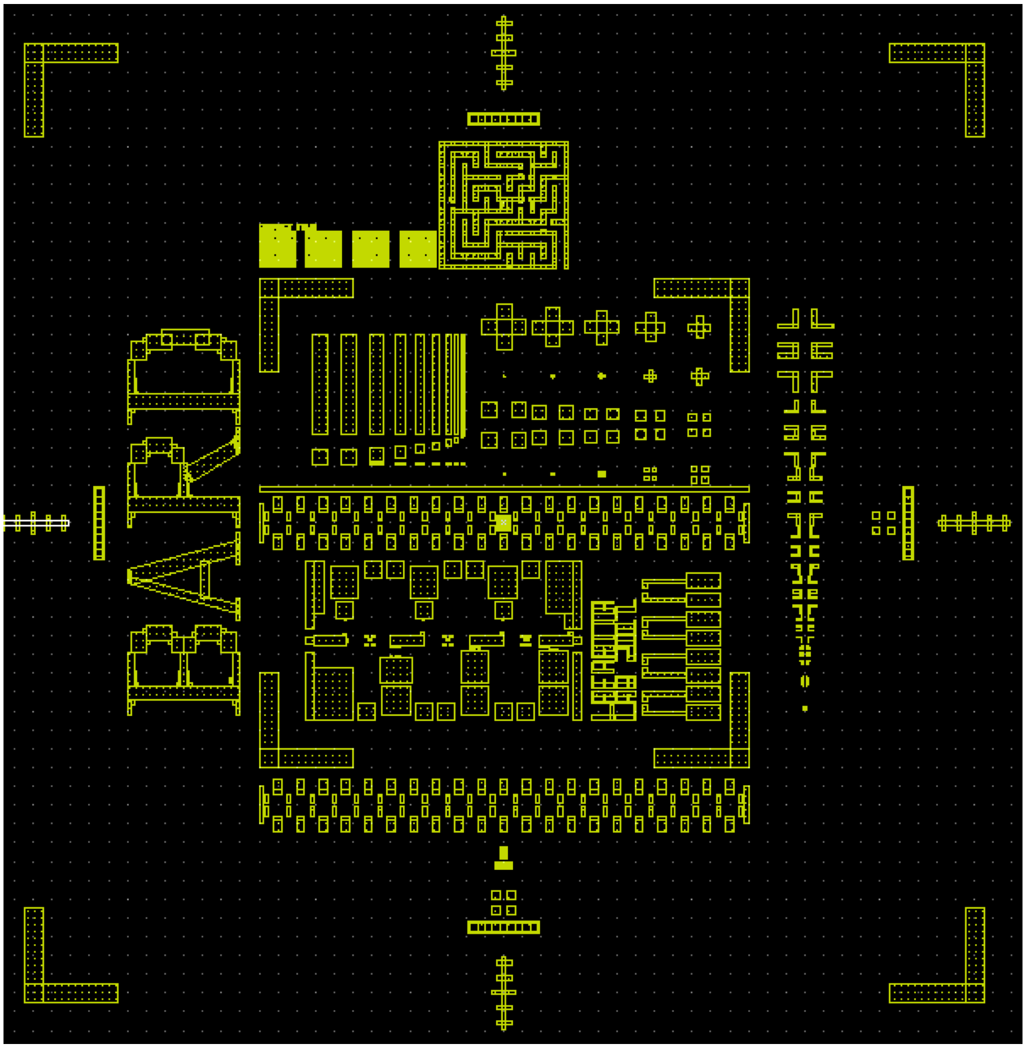

Figure 7: The registration test mask design in LayoutEditor. The "L-shaped" brackets at the edges are 2 inches apart. The inner brackets are 1 inch apart. The smallest feature size is down to 25 μm.

3.5 Sub-micron wide lines can be made by DLW

Using a 20× 0.75 numerical aperture (NA) objective, sub-micron features can be created by our DLW system. Figure 8 shows electron micrographs of some typical lines fabricated at 40 µm/s for S1813 and 10 µm/s for SU-8F. The narrowest lines we could reproducibly write were 780 ± 140 nm wide for S1813 and 950 ± 90 nm for SU-8F. The line height was equal to the film thickness, which was close to 1 µm for S1813 and 5 µm for SU-8F. Other speeds were tested for both photoresists ranging from 5 - 50 µm/s. Faster speeds gave smaller lines that were irreproducible and that sometimes did not develop completely down to the substrate (s1813) or resulted in wavy lines that partially delaminated (SU-8F)

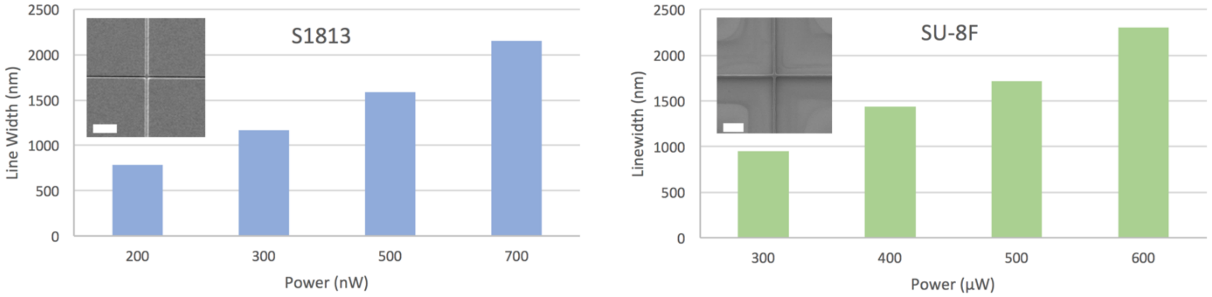

Figure 8: Linewidth data for varying powers using a 20× NA = 0.75 objective. S1813 lines were written at 40 µm/s and SU-8F lines were written at 10 µm/s. The inset show typical SEM micrographs for these samples (scalebars are 10 µm).

<u>3.6 Patterns can be Registered by DLW to Within About 2 µm on Existing Patterns</u>

When performing DLW, the first step is to register the position of existing features that were made during the mask exposure. This is possible because of the contrast between the exposed and unexposed regions and because the DLW system is itself a microscope where we can directly image the sample while simultaneously exposing it. We tested how accurately and precisely we could position the laser beam on the DLW system using a test pattern that contained dozens of rectangles spanning the length of the mask. By drawing lines from the center of one rectangle to the next and measuring the distance of the line from the center point, we obtained measurements for Δx (horizontal) or Δy (vertical). Figure 9 shows a schematic of a portion of the mask and how we define Δx and Δy. Δx (or Δy) is calculated by measuring the distance of the line to both edges of the rectangle then the difference between these numbers is divided by two (Figure. 9c). If the line is perfectly centered then both distances to the edge will be the same and Δx will be 0. We define the radius, Δr, within which we can position the laser focal point as $\Delta r = (\Delta x^2 + \Delta y^2)^{½}$. Hundreds of lines were measured on more than a dozen different wafers to give and an average Δr of 1.6 ± 1.4 µm for S1813 and 2.2 ± 1.5 µm for SU-8F. These numbers are reasonable given the accuracy and precision of the transparency mask. We believe the Δr is slightly smaller for S1813 because its contrast is more pronounced than that of SU-8F, making it easier to pinpoint the edge of an exposed area. Since the use of a mask in LAMP is intended to pattern large features quickly, it is likely the case that registering smaller features to within about 2 µm is sufficiently accurate; if it is not, then more intermediate sized features can be made by DLW to better marry the large-scale pattern to the smaller scale.

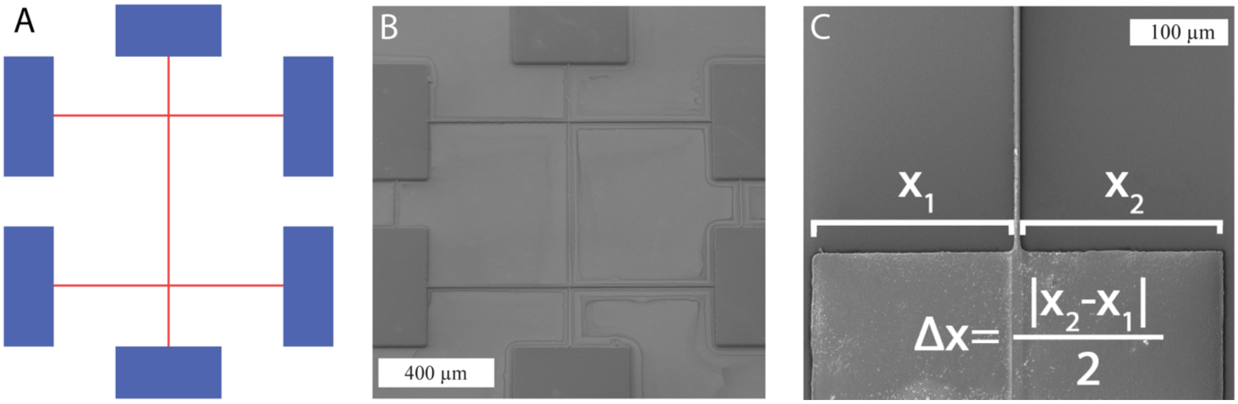

Figure 9: (A) Schematic of the rectangles on the mask that were used for registration marks. The thin red lines were drawn with the laser and their distance from the center of the rectangle, either Δx or Δy, was measured by imaging with the SEM. (B) Typical set of laser augmented registration lines. (C) Close-up of a registration rectangle showing how Δx was measured and calculated

3.7 Proof of Principle Structures

In addition to the characterization samples for linewidth and registration we also used LAMP to make two proof-of-principle devices, one each for the positive- and negative-tone photoresists. S1813 was used to pattern a simple interdigitated electrode have large contact wires that lead into electrodes that are 3 μm wide. The SU-8F was used to create a microfluidic chip having both large channels and very small ones that act as a filter to trap objects like beads and cells.

3.7.1 Interdigitated electrode

Interdigitated electrodes (IDEs) are planar capacitors with high surface area and are useful for electrochemical impedance spectroscopy (Ohno et. al. 2013). The IDE we fabricated by LAMP occupies an area of approximately 200 × 200 µm and took only a couple of minutes to pattern. The IDE was connected to leads that were over a centimeter long and were made by a mask exposure. Had these leads been made with the laser it would have taken hours to expose such a large area even if the speeds and powers were doubled. Following LAMP, the IDE sample was gold coated and liftoff was performed leaving the electrode on glass, which was imaged by reflectance microscopy (Figure 10). The inset image in Figure 10 shows that the individual lines are about 3 µm wide, 200 µm long, and spaced 12.5 µm apart. Such IDEs have been used in microfluidic channels for electrochemical impedance spectroscopy of cells and bacteria (Varshney et. al. 2009; Wang et. al. 2009; Dweik et. al. 2012)

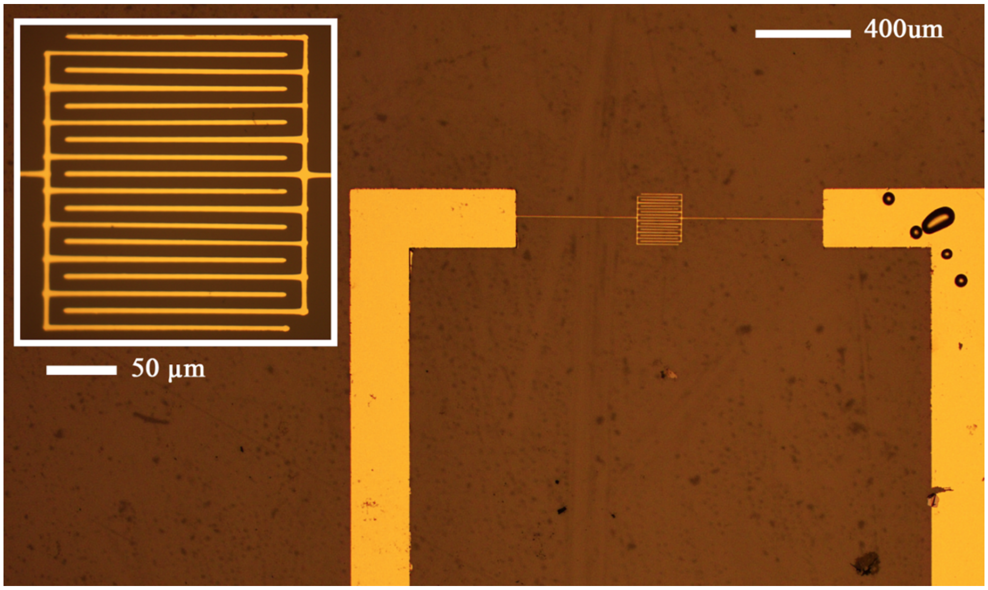

Figure 10: Optical micrograph in reflectance mode of an interdigitated electrode (IDE) patterned by LAMP using S1813 photoresist. The inset shows a close-up view of the same IDE.

3.7.2 Cell Trapping Microfluidic

Another application of LAMP using the negative tone resist SU-8F is for the creation of microfluidic masters. A cell trapping array was fabricated by using a mask for an IDE like pattern and the laser was used to define 2 µm channels between the prongs. Following development and PDMS molding, the mold was bonded to a glass slide. The result was micron-scale channels in the location where the SU-8F was polymerized. 5 µm silica beads were flowed in an aqueous solution through these channels and were trapped at the intersection points between the laser drawn channels and the larger mask patterned channels (Figure 11). As with other examples of soft lithography, the master could be used repeatedly to generate new microfluidic molds. We used another mold to trap *S. cerevisia* cells in a similar device. Devices that create arrays like this could be useful for multiplexed single-cell assays, for size sorting particles or cells, or for mechanical deformability assays of cells (Wlodkowic et. al. 2009).

The power of LAMP is that making and testing these types of devices is very quick because the variable features, which are written with the laser, can be made in minutes and the lead-in channels, and the features which are made with the mask, need not change between prototypes. Thus LAMP enables prototyping with the “fail fast” mantra to quickly troubleshoot and optimize a design before committing to an expensive mask for mass production.

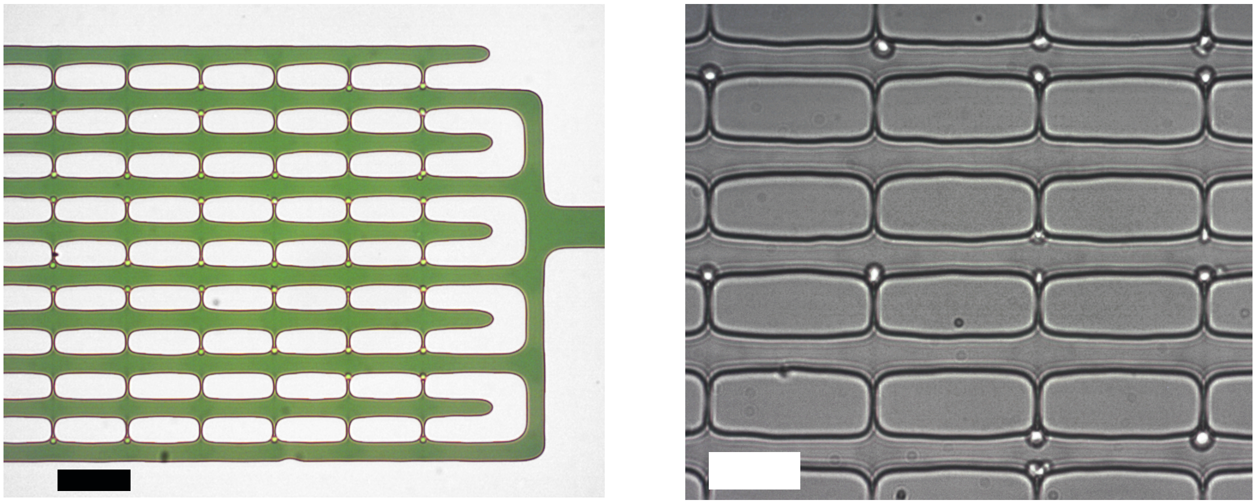

Figure 11: The image on the left shows an array of trapped 5 μm diameter silica beads in a PDMS microfluidic device containing green dyed water (scale bar is 50 μm). The right image shows an array of trapped *S. cerevisia* cells in a similar device (scale bar is 30 μm).

4. CONCLUSION

In this work, we demonstrated a new hybrid lithography technique that combines conventional mask-based UV lithography with DLW to compensate for the drawbacks of each. Using Laser Augmented Microlithographic Patterning, LAMP, we showed that sub-micron laser written features could be registered to larger mask patterns to within about 2 μm in both positive- and negative-tone photoresist. We demonstrated an interdigitated electrode and a microfluidic device as typical examples of our LAMP technique. We hope that others who have access to a DLW system, will consider using it to augment conventional lithography to increase the speed and efficiency with which they can generate their samples.

6.1 APPENDIX A: S1813 Linewidth Data

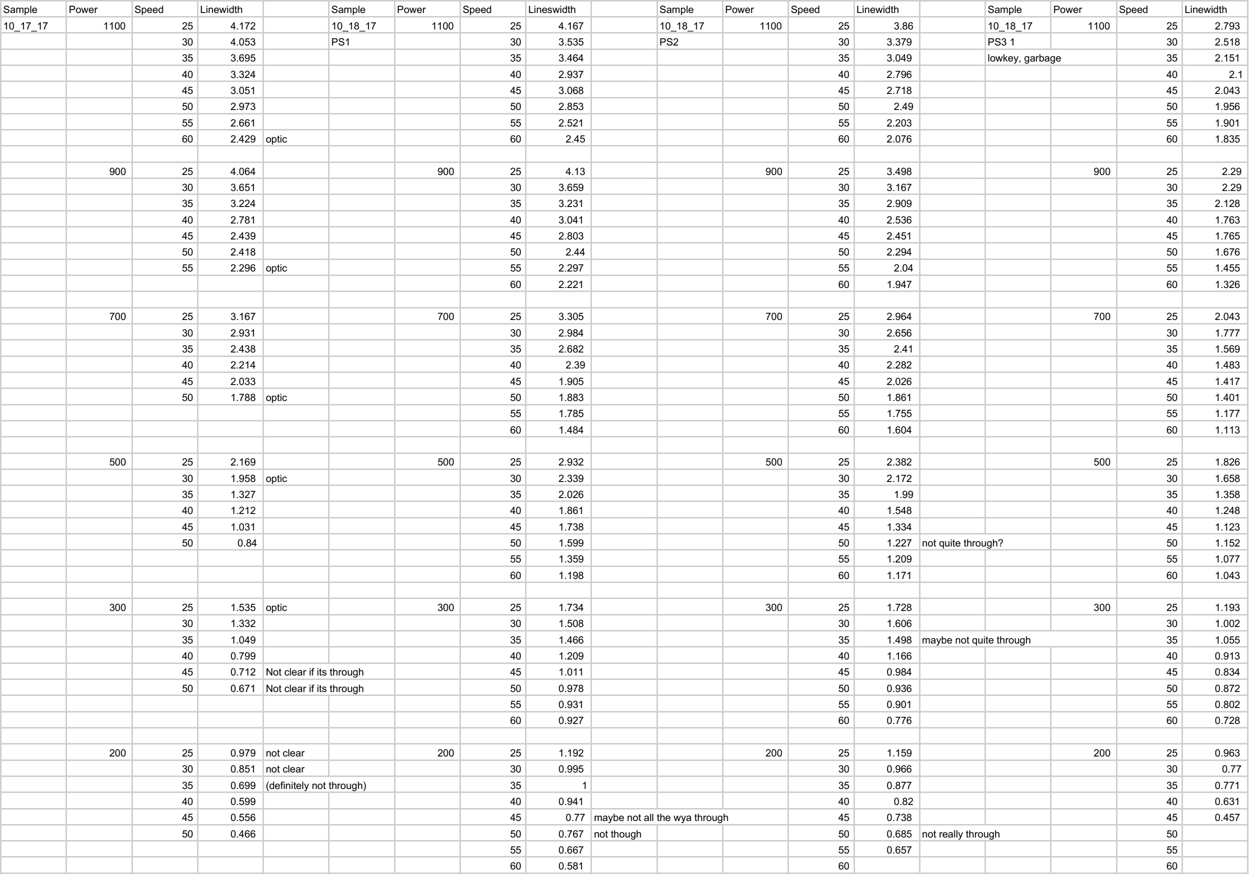

Sample	Power	Speed	Linewidth		Sample	Power	Speed	Lineswidth		Sample	Power	Speed	Linewidth		Sample	Power	Speed	Linewidth
10_17_17	1100	25	4.172		10_18_17	1100	25	4.167		10_18_17	1100	25	3.86		10_18_17	1100	25	2.793
		30	4.053		PS1		30	3.535		PS2		30	3.379		PS3 1		30	2.518
		35	3.695				35	3.464				35	3.049		lowkey, garbage		35	2.151
		40	3.324				40	2.937				40	2.796				40	2.1
		45	3.051				45	3.068				45	2.718				45	2.043
		50	2.973				50	2.853				50	2.49				50	1.956
		55	2.661				55	2.521				55	2.203				55	1.901
		60	2.429	optic			60	2.45				60	2.076				60	1.835
	900	25	4.064			900	25	4.13			900	25	3.498			900	25	2.29
		30	3.651				30	3.659				30	3.167				30	2.29
		35	3.224				35	3.231				35	2.909				35	2.128
		40	2.781				40	3.041				40	2.536				40	1.763
		45	2.439				45	2.803				45	2.451				45	1.765
		50	2.418				50	2.44				50	2.294				50	1.676
		55	2.296	optic			55	2.297				55	2.04				55	1.455
							60	2.221				60	1.947				60	1.326
	700	25	3.167			700	25	3.305			700	25	2.964			700	25	2.043
		30	2.931				30	2.984				30	2.656				30	1.777
		35	2.438				35	2.682				35	2.41				35	1.569
		40	2.214				40	2.39				40	2.282				40	1.483
		45	2.033				45	1.905				45	2.026				45	1.417
		50	1.788	optic			50	1.883				50	1.861				50	1.401
							55	1.785				55	1.755				55	1.177
							60	1.484				60	1.604				60	1.113
	500	25	2.169			500	25	2.932			500	25	2.382			500	25	1.826
		30	1.958	optic			30	2.339				30	2.172				30	1.658
		35	1.327				35	2.026				35	1.99				35	1.358
		40	1.212				40	1.861				40	1.548				40	1.248
		45	1.031				45	1.738				45	1.334				45	1.123
		50	0.84				50	1.599				50	1.227	not quite through?			50	1.152
							55	1.359				55	1.209				55	1.077
							60	1.198				60	1.171				60	1.043
	300	25	1.535	optic		300	25	1.734			300	25	1.728			300	25	1.193
		30	1.332				30	1.508				30	1.606				30	1.002
		35	1.049				35	1.466				35	1.498	maybe not quite through			35	1.055
		40	0.799				40	1.209				40	1.166				40	0.913
		45	0.712	Not clear if its through			45	1.011				45	0.984				45	0.834
		50	0.671	Not clear if its through			50	0.978				50	0.936				50	0.872
							55	0.931				55	0.901				55	0.802
							60	0.927				60	0.776				60	0.728
	200	25	0.979	not clear		200	25	1.192			200	25	1.159			200	25	0.963
		30	0.851	not clear			30	0.995				30	0.966				30	0.77
		35	0.699	(definitely not through)			35	1				35	0.877				35	0.771
		40	0.599				40	0.941				40	0.82				40	0.631
		45	0.556				45	0.77	maybe not all the wya through			45	0.738				45	0.457
		50	0.466				50	0.767	not though			50	0.685	not really through			50	
							55	0.667				55	0.657				55	
							60	0.581				60					60	

Sample	Power	Speed	Linewidth		Sample	Power	Speed	Linewidth		Sample	Power	Speed	Linewidth		Average	std dev		Speed	Power	nm	Line Width	Std Dev	1000
10_18_17	1100	25	2.837		10_18_17	1100	25	4.56		10_18_17	1100	25	4.493		3.840285714	0.68291177		25	200	1105	1.10500000	0.13778969	137.789695
PS3 2		30	2.681		PS4 1		30	4.025		PS4 2		30	4.131		3.474571429	0.67610146			300	1621.71429	1.62171429	0.21969441	219.694407
		35	2.439				35	3.627				35	4.027		3.207428571	0.65838684			500	2383.42857	2.38342857	0.41434349	414.343494
		40	2.324				40	3.353				40	3.53		2.909142857	0.52632747			700	2987	2.98700000	0.50981201	509.81201
		45	1.995				45	3.152				45	3.137		2.737714286	0.48787727			900	3503	3.50300000	0.77847892	778.47892
		50	1.937				50	2.94				50	3.06		2.601285714	0.45581066			1100	3840.28571	3.84028571	0.68291177	682.911773
		55	1.84				55	2.796				55	2.989		2.415857143	0.42227566				0			0
		60	1.6				60	2.717				60	2.731		2.262571429	0.41748705		30	200	918.571429	0.91857143	0.12992588	129.92588
																			300	1413.57143	1.41357143	0.242254	242.253999
	900	25	2.354			900	25	3.938			900	25	4.247		3.503000000	0.77847892			500	2146.42857	2.14642857	0.30256642	302.566418
		30	2.348				30	3.764				30	3.785		3.237714286	0.61731672			700	2656.85714	2.65685714	0.50365227	503.65227
		35	2.311				35	3.352				35	3.409		2.937714286	0.52539937			900	3237.71429	3.23771429	0.61731672	617.316724
		40	2.077				40	3.08				40	3.23		2.644000000	0.53124735			1100	3474.57143	3.47457143	0.67610146	676.101462
		45	2.011				45	2.81				45	2.723		2.428857143	0.41210822				0			0
		50	1.766				50	2.575				50	2.718		2.269571429	0.38850915		35	200	872.428571	0.87242857	0.10567965	105.679646
		55	1.569				55	2.557				55	2.579		2.113285714	0.41868813			300	1349.57143	1.34957143	0.22609453	226.094525
		60	1.497				60	2.289				60	2.374		1.942333333	0.42865585			500	1794.71429	1.79471429	0.38676341	386.763413
																			700	2354.71429	2.35471429	0.43962752	439.627523
	700	25	2.451			700	25	3.459			700	25	3.52		2.987000000	0.50981201			900	2937.71429	2.93771429	0.52539937	525.399372
		30	2.182				30	3.038				30	3.03		2.656857143	0.50365227			1100	3207.42857	3.20742857	0.65838684	658.386842
		35	1.969				35	2.655				35	2.76		2.354714286	0.43962752				0			0
		40	1.811				40	2.471				40	2.407		2.151142857	0.35884343		40	200	784.571429	0.78457143	0.13132159	131.321588
		45	1.615				45	2.301				45	2.096		1.913285714	0.3198144			300	1167	1.16700000	0.28529404	285.294037
		50	1.744				50	2.119				50	2.082		1.839714286	0.25727463			500	1583.85714	1.58385714	0.35566733	355.667331
		55	1.676				55	2.089				55	1.974		1.742666667	0.29790308			700	2151.14286	2.15114286	0.35884343	358.843433
		60	1.484				60	1.835				60	1.856		1.562666667	0.29615316			900	2644	2.64400000	0.53124735	531.247353
																			1100	2909.14286	2.90914286	0.52632747	526.327474
	500	25	1.876			500	25	2.653			500	25	2.846		2.383428571	0.41434349				0			0
		30	2.012				30	2.475				30	2.411		2.146428571	0.30256642		45	200	716.571429	0.71657143	0.15698408	156.984076
		35	1.576				35	2.133				35	2.153		1.794714286	0.38676341			300	962.285714	0.96228571	0.24524678	245.246783
		40	1.269				40	2.06				40	1.889		1.583857143	0.35566733			500	1389.71429	1.38971429	0.34837982	348.379821
		45	1.166				45	1.824				45	1.512		1.389714286	0.34837982			700	1913.28571	1.91328571	0.31981440	319.814399
ugh		50	1.187				50	1.717				50	1.409		1.304428571	0.30879724			900	2428.85714	2.42885714	0.41210822	412.108223
		55	1.056				55	1.348				55	1.173		1.203666667	0.21032152			1100	2737.71429	2.73771429	0.48787727	487.877274
		60	1.08				60	1.255				60	1.369		1.186000000	0.11513896				0			0
																		50	200	693	0.69300000	0.14045015	140.450151
	300	25	1.472			300	25	1.861			300	25	1.829		1.621714286	0.21969441			300	921.428571	0.92142857	0.14521966	145.219661
		30	1.29				30	1.542				30	1.615		1.413571429	0.242254			500	1304.42857	1.30442857	0.30879724	308.797238
		35	1.17				35	1.633				35	1.576		1.349571429	0.22609453			700	1839.71429	1.83971429	0.25727463	257.274628
		40	1.049				40	1.541				40	1.492		1.167000000	0.28529404			900	2269.57143	2.26957143	0.38850915	388.50915
		45	0.851				45	1.118				45	1.226		0.962285714	0.24524678			1100	2601.28571	2.60128571	0.45581066	455.810662
		50	0.827				50	1.134				50	1.032		0.921428571	0.14521966				0			0
		55	0.799				55	1.091				55	0.952		0.912666667	0.12010676		55	200	655.6	0.65560000	0.12703597	127.035975
		60	0.751				60	0.909				60	0.927		0.836333333	0.11950459			300	912.666667	0.91266667	0.12010676	120.106755
																			500	1203.66667	1.20366667	0.21032152	210.321523
	200	25	0.923			200	25	1.207			200	25	1.312		1.105000000	0.13778969			700	1742.66667	1.74266667	0.29790308	297.90308
		30	0.829				30	0.971				30	1.048		0.918571429	0.12992588			900	2113.28571	2.11328571	0.41868813	418.68813
		35	0.813				35	0.963				35	0.984		0.872428571	0.10567965			1100	2415.85714	2.41585714	0.42227566	422.275662
		40	0.728				40	0.852				40	0.921		0.784571429	0.13132159				0			0
		45	0.66				45	0.899				45	0.936		0.716571429	0.15698408		60	200	649.333333	0.64933333	0.08321471	83.2147072
		50	0.602				50	0.867	not through			50	0.771		0.693000000	0.14045015			300	836.333333	0.83633333	0.11950459	119.50459
		55	0.465				55	0.805				55	0.684		0.655600000	0.12703597			500	1186	1.18600000	0.11513896	115.138958
		60					60	0.648	just a dot			60	0.719		0.649333333	0.08321471			700	1562.66667	1.56266667	0.29615316	296.153159
															standard devations				900	1942.33333	1.94233333	0.42865585	428.655849
															0.13546569				1100	2262.57143	2.26257143	0.41748705	417.487051

6.2 APPENDIX B: SU-8F Registration Data

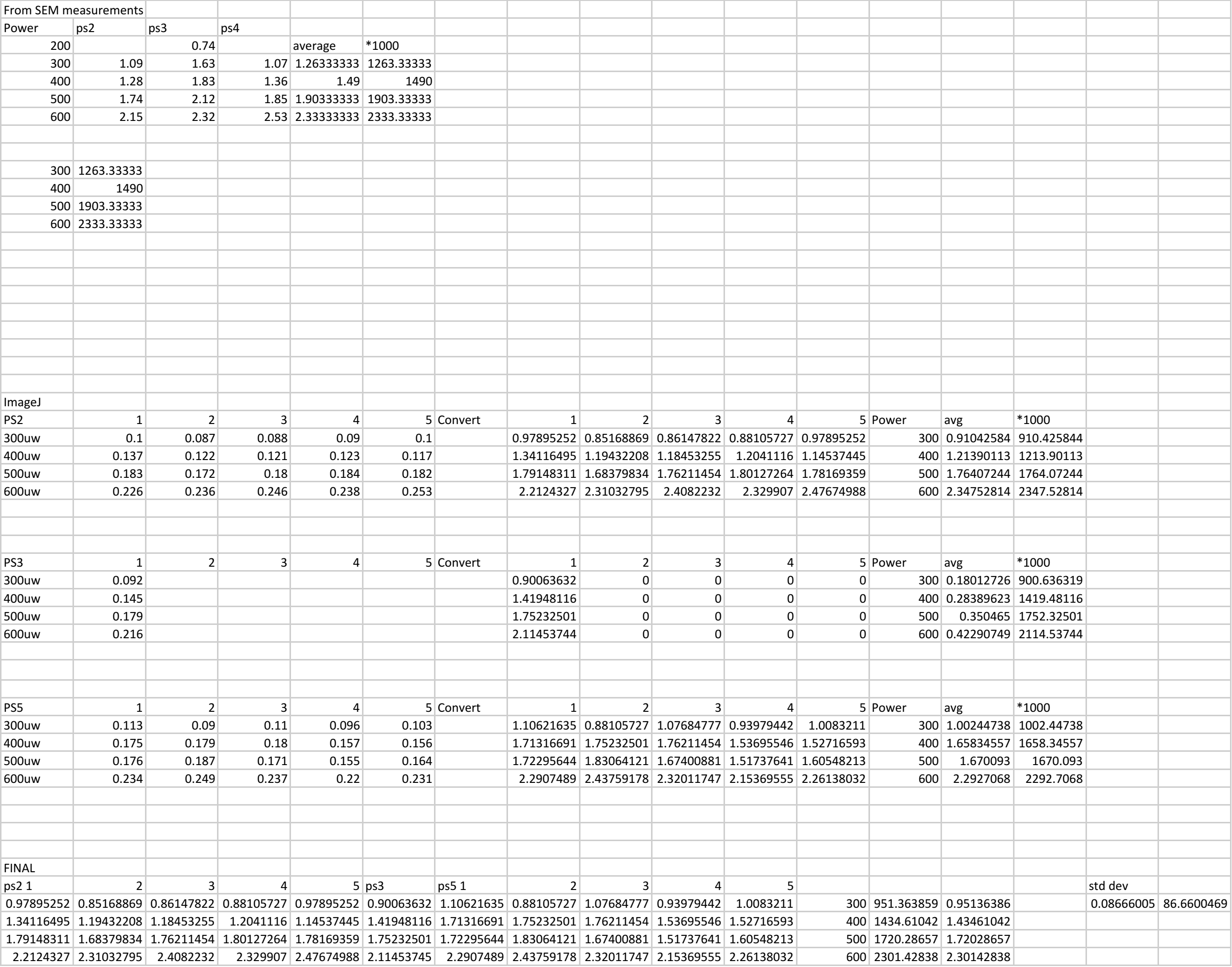

From SEM measurements					
Power	ps2	ps3	ps4		
200		0.74		average	*1000
300	1.09	1.63	1.07	1.26333333	1263.33333
400	1.28	1.83	1.36	1.49	1490
500	1.74	2.12	1.85	1.90333333	1903.33333
600	2.15	2.32	2.53	2.33333333	2333.33333

300	1263.33333
400	1490
500	1903.33333
600	2333.33333

ImageJ														
PS2	1	2	3	4	5	Convert	1	2	3	4	5	Power	avg	*1000
300uw	0.1	0.087	0.088	0.09	0.1		0.97895252	0.85168869	0.86147822	0.88105727	0.97895252	300	0.91042584	910.425844
400uw	0.137	0.122	0.121	0.123	0.117		1.34116495	1.19432208	1.18453255	1.2041116	1.14537445	400	1.21390113	1213.90113
500uw	0.183	0.172	0.18	0.184	0.182		1.79148311	1.68379834	1.76211454	1.80127264	1.78169359	500	1.76407244	1764.07244
600uw	0.226	0.236	0.246	0.238	0.253		2.2124327	2.31032795	2.4082232	2.329907	2.47674988	600	2.34752814	2347.52814

PS3	1	2	3	4	5	Convert	1	2	3	4	5	Power	avg	*1000
300uw	0.092						0.90063632	0	0	0	0	300	0.18012726	900.636319
400uw	0.145						1.41948116	0	0	0	0	400	0.28389623	1419.48116
500uw	0.179						1.75232501	0	0	0	0	500	0.350465	1752.32501
600uw	0.216						2.11453744	0	0	0	0	600	0.42290749	2114.53744

PS5	1	2	3	4	5	Convert	1	2	3	4	5	Power	avg	*1000
300uw	0.113	0.09	0.11	0.096	0.103		1.10621635	0.88105727	1.07684777	0.93979442	1.0083211	300	1.00244738	1002.44738
400uw	0.175	0.179	0.18	0.157	0.156		1.71316691	1.75232501	1.76211454	1.53695546	1.52716593	400	1.65834557	1658.34557
500uw	0.176	0.187	0.171	0.155	0.164		1.72295644	1.83064121	1.67400881	1.51737641	1.60548213	500	1.670093	1670.093
600uw	0.234	0.249	0.237	0.22	0.231		2.2907489	2.43759178	2.32011747	2.15369555	2.26138032	600	2.2927068	2292.7068

FINAL																
ps2 1	2	3	4	5	ps3	ps5 1	2	3	4	5					std dev	
0.97895252	0.85168869	0.86147822	0.88105727	0.97895252	0.90063632	1.10621635	0.88105727	1.07684777	0.93979442	1.0083211	300	951.363859	0.95136386		0.08666005	86.6600469
1.34116495	1.19432208	1.18453255	1.2041116	1.14537445	1.41948116	1.71316691	1.75232501	1.76211454	1.53695546	1.52716593	400	1434.61042	1.43461042			
1.79148311	1.68379834	1.76211454	1.80127264	1.78169359	1.75232501	1.72295644	1.83064121	1.67400881	1.51737641	1.60548213	500	1720.28657	1.72028657			
2.2124327	2.31032795	2.4082232	2.329907	2.47674988	2.11453745	2.2907489	2.43759178	2.32011747	2.15369555	2.26138032	600	2301.42838	2.30142838			

6.3 APPENDIX C: S1813 Registration Data

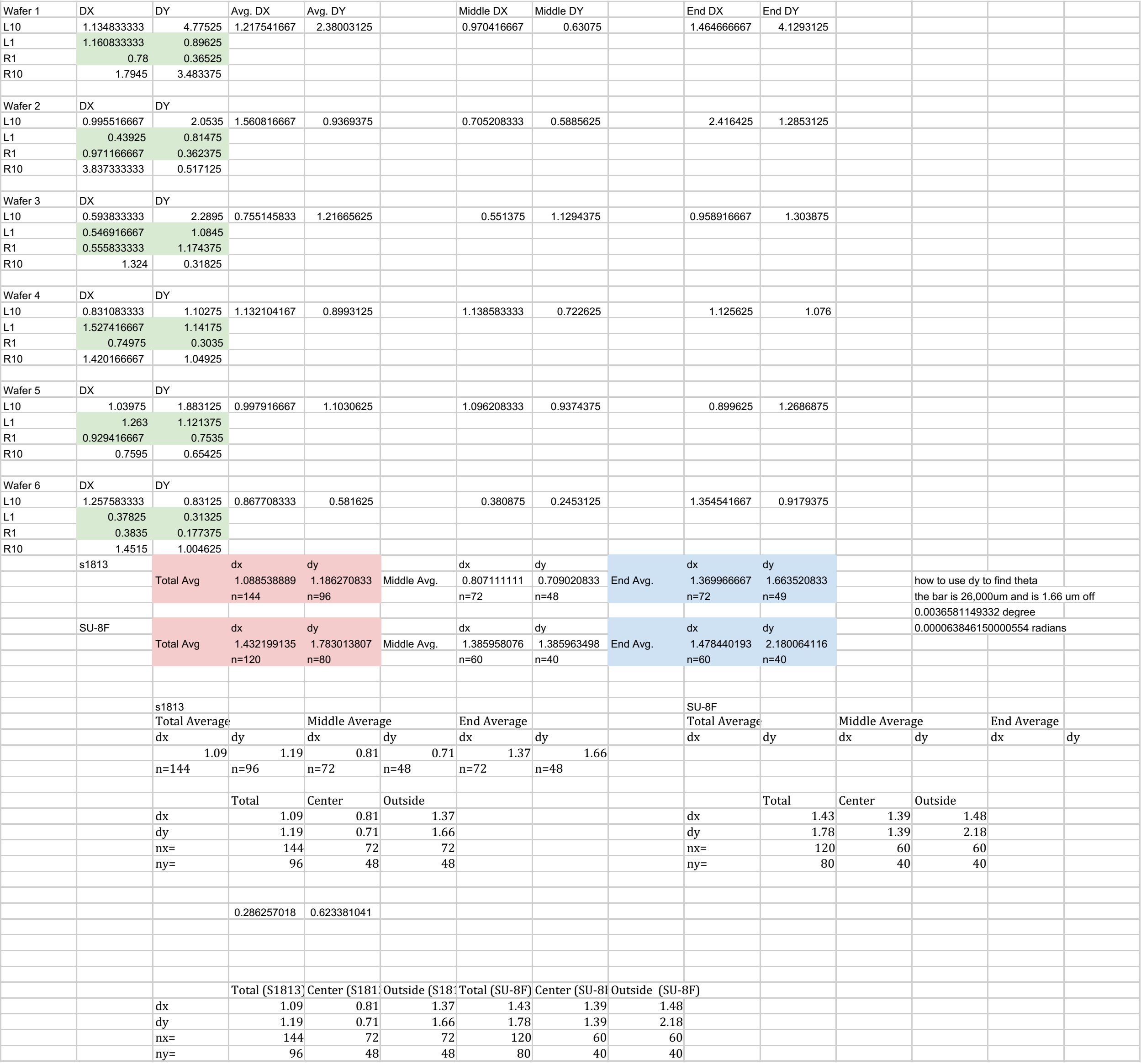

Wafer 1	DX	DY	Avg. DX	Avg. DY		Middle DX	Middle DY		End DX	End DY				
L10	1.134833333	4.77525	1.217541667	2.38003125		0.970416667	0.63075		1.464666667	4.1293125				
L1	1.160833333	0.89625												
R1	0.78	0.36525												
R10	1.7945	3.483375												
Wafer 2	DX	DY												
L10	0.995516667	2.0535	1.560816667	0.9369375		0.705208333	0.5885625		2.416425	1.2853125				
L1	0.43925	0.81475												
R1	0.971166667	0.362375												
R10	3.837333333	0.517125												
Wafer 3	DX	DY												
L10	0.593833333	2.2895	0.755145833	1.21665625		0.551375	1.1294375		0.958916667	1.303875				
L1	0.546916667	1.0845												
R1	0.555833333	1.174375												
R10	1.324	0.31825												
Wafer 4	DX	DY												
L10	0.831083333	1.10275	1.132104167	0.8993125		1.138583333	0.722625		1.125625	1.076				
L1	1.527416667	1.14175												
R1	0.74975	0.3035												
R10	1.420166667	1.04925												
Wafer 5	DX	DY												
L10	1.03975	1.883125	0.997916667	1.1030625		1.096208333	0.9374375		0.899625	1.2686875				
L1	1.263	1.121375												
R1	0.929416667	0.7535												
R10	0.7595	0.65425												
Wafer 6	DX	DY												
L10	1.257583333	0.83125	0.867708333	0.581625		0.380875	0.2453125		1.354541667	0.9179375				
L1	0.37825	0.31325												
R1	0.3835	0.177375												
R10	1.4515	1.004625												
	s1813		dx	dy		dx	dy		dx	dy				
		Total Avg	1.088538889	1.186270833	Middle Avg.	0.807111111	0.709020833	End Avg.	1.369966667	1.663520833		how to use dy to find theta		
			n=144	n=96		n=72	n=48		n=72	n=49		the bar is 26,000um and is 1.66 um off		
												0.0036581149332 degree		
	SU-8F		dx	dy		dx	dy		dx	dy		0.000063846150000554 radians		
		Total Avg	1.432199135	1.783013807	Middle Avg.	1.385958076	1.385963498	End Avg.	1.478440193	2.180064116				
			n=120	n=80		n=60	n=40		n=60	n=40				
		s1813							SU-8F					
		Total Average		Middle Average		End Average			Total Average		Middle Average		End Average	
		dx	dy	dx	dy	dx	dy		dx	dy	dx	dy	dx	dy
		1.09	1.19	0.81	0.71	1.37	1.66							
		n=144	n=96	n=72	n=48	n=72	n=48							
			Total	Center	Outside					Total	Center	Outside		
		dx	1.09	0.81	1.37				dx	1.43	1.39	1.48		
		dy	1.19	0.71	1.66				dy	1.78	1.39	2.18		
		nx=	144	72	72				nx=	120	60	60		
		ny=	96	48	48				ny=	80	40	40		
			0.286257018	0.623381041										
			Total (S1813)	Center (S181	Outside (S181	Total (SU-8F)	Center (SU-8	Outside (SU-8F)						
		dx	1.09	0.81	1.37	1.43	1.39	1.48						
		dy	1.19	0.71	1.66	1.78	1.39	2.18						
		nx=	144	72	72	120	60	60						
		ny=	96	48	48	80	40	40						

6.4 APPENDIX D: SU-8F Registration Data

B Wafer 1	DX	DY	Avg. DX	Avg. DY		Middle DX	Middle DY		End DX	End DY
L10	1.040875	0.78425	0.917020833	0.8844375		0.793166667	0.984625		1.040875	0.78425
L1	0.793166667	0.984625								
R1										
R10										
B Wafer 2	DX	DY								
L10	1.376	4.048875	0.989833333	3.0761875		0.603666667	2.1035		1.376	4.048875
L1	0.603666667	2.1035								
R1										
R10										
9.21 2	DX	DY								
L10	1.573917931	3.28836425	1.382448004	1.633642496		1.419336706	1.385961214		1.345559303	1.881323777
L1	1.749578415	0.94856661								
R1	1.089094997	1.823355818								
R10	1.117200675	0.474283305								
10.06	DX	DY								
L10	0.920460933	3.319983137	1.22084036	1.920847386		0.95559303	0.685075885		1.48608769	3.156618887
L1	1.250702642	0.853709949								
R1	0.660483418	0.516441821								
R10	2.051714446	2.993254637								
10.10 1	DX	DY								
L10	3.766160764	0.748313659	2.059443508	1.056597808		1.926644182	1.090851602		2.192242833	1.022344013
L1	2.230185497	0.822091062								
R1	1.623102867	1.359612142								
R10	0.618324902	1.296374368								
10.10 2	DX	DY								
L10	1.665261383	3.520236088	2.023608769	2.126370152		2.617341203	2.065767285		1.429876335	2.186973019
L1	3.330522766	2.266020236								
R1	1.90415964	1.865514334								
R10	1.194491287	0.853709949								
			dx	dy		dx	dy		dx	dy
		Total Avg	1.432199135	1.783013807	Middle Avg.	1.385958076	1.385963498	End Avg.	1.478440193	2.180064116
			n=120	n=80		n=60	n=40		n=60	n=40
Outlier										
9.21 1	DX	DY								
L10	7.51826869	18.23355818								
L1	3.632658797	5.111720067								
R1	7.173974143	1.981450253								
R10	4.503934795	11.59359191								

References:

1. P. S. Waggoner and H. G. Craighead, "Micro- and nanomechanical sensors for environmental, chemical, and biological detection," Lab on a Chip 7, 1238–1255 (2007).
2. Y. Xia and G. M. Whitesides, "Soft Lithography," Angewandte Chemie International Edition **37**, 550–575 (1998).
3. C. N. LaFratta and D. R. Walt, "Very high density sensing arrays," Chem. Rev. 108, 614–637 (2008).
4. M. Gersborg-Hansen, L. H. Thamdrup, A. Mironov, and A. Kristensen, "Combined electron beam and UV lithography in SU-8," Microelectronic Engineering 84, 1058–1061 (2007).
5. S. F. A Rahman; U. Hashim; M. N. M. Nor; M. E. A. Shohini*, "Electron beam lithography in ma-N 2403 and optical mixed lithography in PR1-2000A, together on silicon on insulator (SOI)" Journal of Nanoelectronics and Materials* 2011, 4, 49 (2010).
6. H. Nakano; K. Takahashi; A. Kawai, "Negative Pattern Formation in Positive Resist Layer by EB / UV Hybrid Lithography" *Journal of Photopolymer Science and Technology* 29 (4), 603-606 (2016).
7. J. C. Potosky; A. J. Higgins.; S. T. Hoelke.; R. G. Imerson; F. F. Kinoshita; R. L. Maddox.; J. P. Reekstin, "An electron-beam/optical-hybrid lithography approach to submicrometer electronic devices" *Journal of Vacuum Science and Technology 19* (4), 924–926 (1981).

8. D. J. Carbaugh; S. G. Pandya and J. T. Wright and S. Kaya and F. Rahman, " Combination photo and electron beam lithography with polymethyl methacrylate (PMMA) resist"*Nanotechnology 28* (45), 455301 (2017)

9. S. Steen; S. J. McNab; L. Sekaric; I. Babich; J. Patel; J. Bucchignano; M. Rooks; D. M. Fried; A. W. Topol; J. R. Brancaccio.; R. Yu; J. M. Hergenrother; J. P. Doyle; R. Nunes; R. G. Viswanathan; S. Purushothaman; M. B. Rothwell, " Looking into the crystal ball: future device learning using hybrid e-beam and optical lithography (Keynote Paper)" *Microelectronic Engineering 83* (4), 754–761 (2006).

10. L. Mollard.; S. Tedesco; B. Dal'zotto; V. Jaubert.; L. Pain; G. Fanget; C. Comboroure; Y. Morand; M. Fayolle, "Hybrid deep UV–e-beam lithography for the fabrication of dual damascene structures" *Microelectronic Engineering*, *57–58* (Supplement C), 269 275 (2001).

11. F. Benistant; S. Tedesco; G. Guegan; F. Martin; M. Heitzmann; B. Dal'zotto, " A heavy ion implanted pocket 0.10 μm n-type metal–oxide–semiconductor field effect transistor with hybrid lithography (electron-beam/deep ultraviolet) and specific gate passivation process " *Journal of Vacuum Science & Technology B: Microelectronics and Nanometer Structures Processing, Measurement, and Phenomena 14* (6), 4051–4054 (1996).

12. R. Jonckheere; A. Tritchkov.; V. Van Driessche; L. Van den hove, " Electron beam / DUV intra-level mix-and-match lithography for random logic 0.25μm CMOS" *Microelectronic Engineering 27* (1), 231–234 (1995).

13. K. Dhima; C. Steinberg; A. Mayer; S. Wang; S. Möllenbeck; H.C. Scheer, " Reversed order hybrid lithography of T-NIL and UVL" *Microelectronic Engineering 100* (Supplement

C), 37–40 (2012).

14. L. Montelius; B. Heidari; M. Graczyk; L. Maximov; E.L. Sarwe.; T.G. I. Ling, "Nanoimprint- and UV-lithography: Mix&Match process for fabrication of interdigitated nanobiosensors" *Microelectronic Engineering 53* (1), 521–524 (2000).

15. F. Reuther; K. Pfeiffer; M. Fink; G. Gruetzner; H. Schulz; H. Scheer; F. Gaboriau; C. Cardinaud, "Mix and match of nanoimprint and UV lithography" Vol. 4343, pp 4343–4348 (2001).

16. H. C. Scheer.; M. Wissen; N. Bogdanski; S. Möllenbeck; A. Mayer, " Potential and limitations of a T-NIL/UVL hybrid process" *Microelectronic Engineering 87* (5), 851–853 (2010).

17. L. H. D. Skjolding, G. T. Teixidor, J. Emnéus, and L. Montelius, "Negative UV–NIL (NUV–NIL) – A mix-and-match NIL and UV strategy for realisation of nano- and micrometre structures," Microelectronic Engineering 86, 654–656 (2009).

18. C. Eschenbaum, D. Großmann, K. Dopf, S. Kettlitz, T. Bocksrocker, S. Valouch, and U. Lemmer, "Hybrid lithography: Combining UV-exposure and two photon direct laser writing," Optics Express 21, 29921 (2013).

19. M. Muluneh; D. Issadore, " Hybrid soft-lithography/laser machined microchips for the parallel generation of droplets" *Lab on a chip 13* (24), 4750–4754 (2013).

20. M. Muluneh; D. Issadore, " A multi-scale PDMS fabrication strategy to bridge the size mismatch between integrated circuits and microfluidics*" Lab on a chip 14* (23), 4552–4558 (2014).

21. R. Nielson, B. Kaehr, and J. B. Shear, "Microreplication and design of biological architectures using dynamic-mask multiphoton lithography," Small **5**, 120–125

(2009).

22. C. N. LaFratta, O. Simoska, I. Pelse, S. Weng, and M. Ingram, "A convenient direct laser writing system for the creation of microfluidic masters," Microfluidics and Nanofluidics 19, 419–426 (2015).

23. C. N. LaFratta, T. Baldacchini, R. A. Farrer, J. T. Fourkas, M. C. Teich, B. E. A. Saleh, and M. J. Naughton, "Replication of two-photon-polymerized structures with extremely high aspect ratios and large overhangs," The Journal of Physical Chemistry B 108, 11256–11258 (2004).

24. D. C. Duffy, J. C. McDonald, O. J. Schueller, and G. M. Whitesides, "Rapid prototyping of microfluidic systems in poly(dimethylsiloxane)," Anal. Chem. 70, 4974–4984 (1998).

25. R. Sjöback, J. Nygren, and M. Kubista, "Absorption and fluorescence properties of fluorescein," Spectrochimica Acta Part A: Molecular and Biomolecular Spectroscopy 51, L7–L21 (1995).

26. R. Ohno, H. Ohnuki, H. Wang, T. Yokoyama, H. Endo, D. Tsuya, and M. Izumi, "Electrochemical impedance spectroscopy biosensor with interdigitated electrode for detection of human immunoglobulin A," Biosensors and Bioelectronics **40,** 422–426 (2013).

27. M. Varshney, Y. Li "Interdigitated array microelectrodes based impedance biosensors for detection of bacterial cells" Biosens and Bioelectr 24:2951–2960 (2009).

28. L. Wang , H Yin , W. Xing, Z Yu, M. Guo, J. Cheng "Real-time, label-free monitoring of the cell cycle with a cellular impedance sensing chip" Biosens and Bioelectr 25:990–995 (2010).

29. M. Dweik, R.C. Stringer,S.G. Dastider, Y. Wu, M. Almasri, S. Barizuddin Specific and targeted detection of viable Escherichia coli O157:H7 using a sensitive and reusable impedance biosensor with dose and time response studies. Talanta 94:84–89 (2012).

30. D. Wlodkowic, S. Faley, M. Zagnoni, J. P. Wikswo, and J. M. Cooper, "Microfluidic single-cell array cytometry for the analysis of tumor apoptosis," Anal. Chem. 81, 5517–5523 (2009).